

M.I. Airila, J.P. Coad, S. Brezinsek, P. Belo, M. Groth, A. Kirschner,
T. Makkonen, J.D. Strachan, A.M. Widdowson, S. Wiesen,
and JET EFDA contributors

Induced Carbon Deposition by Local Hydrocarbon Injection into Detached Divertor Plasmas in JET

“This document is intended for publication in the open literature. It is made available on the understanding that it may not be further circulated and extracts or references may not be published prior to publication of the original when applicable, or without the consent of the Publications Officer, EFDA, Culham Science Centre, Abingdon, Oxon, OX14 3DB, UK.”

“Enquiries about Copyright and reproduction should be addressed to the Publications Officer, EFDA, Culham Science Centre, Abingdon, Oxon, OX14 3DB, UK.”

The contents of this preprint and all other JET EFDA Preprints and Conference Papers are available to view online free at www.iop.org/Jet. This site has full search facilities and e-mail alert options. The diagrams contained within the PDFs on this site are hyperlinked from the year 1996 onwards.

Induced Carbon Deposition by Local Hydrocarbon Injection into Detached Divertor Plasmas in JET

M.I. Airila¹, J.P. Coad², S. Brezinsek³, P. Belo⁴, M. Groth⁵, A. Kirschner³,
T. Makkonen⁵, J.D. Strachan⁶, A.M. Widdowson², S. Wiesen³,
and JET EFDA contributors*

JET-EFDA, Culham Science Centre, OX14 3DB, Abingdon, UK

¹ Association EURATOM-Tekes, VTT Technical Research Centre of Finland, 02044 VTT, Finland

² Association EURATOM-CCFE, Culham Science Centre, Abingdon, OX14 3DB, UK

³ IEF - Plasmaphysik, Forschungszentrum Jülich, TEC, Association EURATOM-FZJ, Germany

⁴ EURATOM/IST Fusion Association, IPFN, Av. Rovisco Pais 1049-001 Lisbon, Portugal

⁵ Aalto University School of Science and Technology, Association Euratom-Tekes, FI-00076 AALTO, Finland

⁶ PPPL Princeton University, Princeton, NJ 08543, USA

* See annex of F. Romanelli et al, "Overview of JET Results",
(Proc. 22nd IAEA Fusion Energy Conference, Geneva, Switzerland (2008)).

Preprint of Paper to be submitted for publication in Proceedings of the
19th International Conference on Plasma Surface Interactions, San Diego, California, USA.
(24th May 2010 - 28th May 2010)

ABSTRACT.

During the detachment experiments of JET in 2007, just before opening the machine, 1×10^{22} molecules of $^{12}\text{CD}_4$ were injected to the L-mode plasma at the outer strike point in the centre of the horizontal target (LBSRP). The deposited layers were analyzed post mortem after the removal of tiles. The heaviest local deposition is found immediately upstream of the gas inlet, but to downstream there is a larger area of deposition. In total, 3.7×10^{20} deuterium atoms were found locally deposited; if in the deposits the mean $\text{D/C} = 0.4$, then about 10% of the injected carbon was locally deposited. Transport and local deposition of the injected carbon was modeled with the 3D Monte Carlo impurity transport code ERO. The plasma background was generated with the onion-skin solver of the DIVIMP code. The toroidal decay of deposition is reproduced with ERO, but the poloidal transport of carbon is several times weaker than measured. The results indicate that re-erosion of the layer during the attached plasma phases has been significant.

1. INTRODUCTION

Fuel retention due to co-deposition with carbon and beryllium remains a critical issue for ITER. Due to its chemical reactivity with hydrogen, carbon sources are potentially large as long as any plasma-facing components contain carbon. Retention estimates are based on understanding carbon sources and migration pathways. Carbon migration in plasma is a complex process starting from physical or chemical erosion of the surface by particle bombardment, followed by successive ionization and transport under the influence of electromagnetic forces, plasma flow, thermal forces and diffusion. Finally, the eroded or injected particles are deposited on the plasma-facing surfaces, where re-erosion may occur, leading to step-wise migration into remote areas. Upon deposition, significant proportions of hydrogen can be co-deposited in the carbon layers, depending on surface temperature and incoming flux. The diagnostic capabilities for studying the details of migration process are limited: The density distributions of impurity species in the plasma can be obtained in situ by spectroscopy, and the final tracer distribution on plasma-facing components can be measured ex situ by e.g. ion beam techniques. Interpretation of the measurements requires computer simulations. Tracer injection experiments [4] are a useful tool to collect information on material migration and deposition under controlled constant plasma conditions and in a single magnetic configuration. It is customary to use the natural isotope ^{13}C of carbon in carbon machines, but the use of the same tracer has been also successfully continued in ASDEX Upgrade after the transition to the all-tungsten wall [10, 11].

The JET 2007 L-mode detachment experiment was executed close to the end of the experimental campaign just before the usual ^{13}C global tracer experiment. No plasma operation was made after the experiment with the outer strike point on tile 5, thus, close to the injection location. Therefore $^{12}\text{CD}_4$ was injected and the deposition analysed by post mortem methods. In the absence of isotopically labeled carbon, the deposited amount was deduced from measured deuterium. A toroidal profile and several poloidal profiles were measured over the deposition area. We have set up a model based on the DIVIMP and ERO codes to explain the local migration. We initiated the deposition modelling

with ERO by assuming a uniform plasma background and scanning density and temperature over the relevant ranges suggested by the uncertainties in the local measurements. This simplified model does not reproduce the deposited fraction and a correct toroidal distribution simultaneously. Therefore we applied the Onion-Skin Model (OSM) of the DIVIMP code [3] to produce a more realistic plasma background for ERO modelling.

This paper is organized as follows: In Section 2 we describe the plasma configurations and post mortem analysis results. Modeling consists of two parts – background plasma generation and impurity migration modeling – and is presented in Section 3. Finally we summarize and discuss the results in Section 4.

2. EXPERIMENT

The experiment is described in [1] and we summarize here the features relevant for impurity modelling at the outer target. A plasma configuration with very asymmetric divertor legs was executed to detach the outer divertor leg using strong deuterium injection through a circumferential Gas Injection Module at the inner divertor (GIM11, see figure 1). The injection was ramped up, resulting in detachment that was observed as the roll-over of the ion flux measured by Langmuir probes and spectroscopically monitored volume recombination of deuterium. The outer strike point was fixed to the center of the Load-Bearing Septum Replacement Plate (LBSRP) where a single Gas Injection Module (GIM14) was used to inject methane ($^{12}\text{CD}_4$) into the detached phases of the plasma. Hydrocarbon injection was performed with the primary goal of investigating chemical sputtering of Carbon-Fibre Composites (CFC) in detached plasma conditions in the outer divertor. Two plasma scenarios in L-mode were executed: at the beginning density ramps to determine the attached and detached plasma regime and feedback-controlled plasmas in detached plasma conditions. The experiment was performed just prior to the end of the campaign and no discharges were run with the outer strike point at the horizontal target during the rest of the campaign. Therefore it is reasonable to assume that the deposition has remained intact and is only attributed to this experiment. After the removal of the tiles, the deuterium content on the surface was analysed with Rutherford Backscattering Spectrometry (RBS). Assuming that the hydrocarbon layer would have a D/C fraction of 0.4, the result is that about 10% of the injected C was deposited locally and remained after the experiment.

The deposition footprint is shown in figure 2 and the poloidal profiles from RBS along three lines on the upstream side tile LB14WR and two poloidal profiles on the downstream tile LB14NL in figure 3. Heavy but very localized deposition is seen upstream from the injection valve. The measured region begins at the very edge of the upstream tile LB14WR (1mm from the edge), where the highest concentration of D ($> 50 \times 10^{18} \text{ cm}^{-2}$) is found.

The concentration falls off to negligible values over a distance of about 1cm. Due to the proximity of the edge and the distance to the gas inlet that is relatively large in this scale we did not attempt to model this part in detail.

On the downstream side, the toroidal decay length of the deposited surface concentration is about

40mm. From the B field inclination with respect to the target surface (about 1/40) one can estimate the ionization length in the plasma to be about 1mm. This implies that only the plasma conditions very close to the target are significant for impurity migration. The profiles at 10 and 28mm from the tile edge show a double maximum, visible also in the photo. One possible explanation is strong re-erosion of the deposit at the strike point during the attached phase, having a peaked flux profile and the strike point lying at the injector location.

3. MODELING

3.1 BACKGROUND PLASMA MODELING

ERO uses the test particle approach to model the 3D transport of impurities in a prescribed plasma background, usually assumed toroidally symmetric and therefore 2D. The simplest approach is to assume uniform background plasma for test impurity tracing. In the present work we performed a parameter scan with uniform plasma parameters spanning the range of uncertainty in the measurements ($3\text{eV} \leq T_e \leq 10\text{eV}$, $10^{19}\text{m}^{-3} \leq n_e \leq 10^{20}\text{m}^{-3}$ and $M = 1$ assumed for the flow velocity). Locally deposited amount consistent with the measured fraction of 10% of the injection was found with the plasma density of $n_e = 3 \times 10^{19}\text{m}^{-3}$ and temperature of $T_e = 3\text{eV}$, but the measured deposition pattern cannot be explained using this simple model. Therefore a more detailed modelling of the plasma background was undertaken, starting from the available Langmuir probe data. The Onion-Skin Model (OSM) of DIVIMP uses target profiles as boundary condition and integrates 1D conservation equations upwards along individual flux tubes. The resulting solution automatically matches the target conditions, unlike fluid plasma solutions, that are usually based on boundary conditions given upstream at the outer midplane and integrated in 2D down to the target. In OSM modelling one has to simplify the cross-field flows remarkably and any complicated cross-field flow patterns are out of reach of OSM modelling. For this work the Onion-Skin Model was selected as the migration was estimated to take place mostly within 1 mm from the target.

To represent the various plasma conditions encountered during the gradually progressing detachment in these experiments, we could feed target data from any time point to the OSM solver as the boundary condition. However, two specific time moments were selected as the injection always occurred in the detached phase, which then should determine the migration. The opposite end, the fully attached phase, was also simulated to obtain the plasma solution for estimating possible re-erosion of the deposited layer during the attached phases of subsequent discharges. The target n_e and T_e profiles for these phases are shown in figure 3 of [1]. For the local flow velocity we used a simple approximation by setting either $M = 1$ or $M = 0.5$ according to the local electron temperature everywhere in the simulation volume. The ion flux corresponding to the two plasma solutions is shown in figure 4. Neutrals will also contribute to the erosion but were not yet included in modeling.

3.2 IMPURITY MODELING

Given the various uniform and OSM generated background plasmas, the 3D Monte Carlo impurity transport code ERO [2] was used to model the local transport of sputtered and injected impurities in

the divertor. We neglected the poloidal gap where the gas injection module GIM14 is located and assumed that the exposed surface is perfectly planar and inclined as shown in figure 1. Since the deposition was rather localised, we used a small simulation volume [50mm in x direction (major radius), 200mm in y (toroidal) and 100mm in z (vertical)], allowing a spatial resolution of 1mm with reasonable computation time. 4000 test particles per time step were used to describe the injection and 10 000 test particles per time step for eroded particles. Close to the injection location, this number of test particles is sufficient, but the deposited density drops off rapidly – especially poloidally – and the pattern is very noisy at the boundaries. The deposition was averaged over neighboring surface cells to improve the readability of figures. The Homogeneous Material Mixing (HMM) surface model of ERO assumes that the influx of particles is immediately mixed into an “interaction layer”, and correspondingly the erosion outflux originates from this layer in proportions given by the relative concentrations of different species. The interaction layer thickness was 5mm and the time step ranged between 0.003s and 0.015s depending on the plasma background (the maximum flux dictates how large time steps can be used without eroding the complete interaction layer). For surface interactions, the following assumptions are rather standard among several recent studies with the ERO code and were used also here: Chemical erosion yield was fixed to 2%, physical sputtering yield is calculated using the Bohdansky and Yamamura formulae, the reflection coefficient for ions and atoms is taken from the TRIM database whereas for hydrocarbons negligible effective sticking is assumed by putting the sticking coefficient $S=0$. There is evidence from QMB measurements at JET [5] and modelling of limiter and divertor tracer injection with the ERO code [6–9] that the re-erosion of deposited layers is considerably enhanced in comparison to pure graphite. In present modelling the erosion of deposited layer was taken in the high end of the possible range with an enhancement factor $f_{re} = 10$ to resolve re-erosion maximally during the attached plasma phase.

We treated separately the attached and detached phases of the discharge. Initially the simulation was run with the detached plasma background and CD4 injection until the net deposition saturated into a steady state value – this was 54% for the $M=1$ case and 58% for $M = 0.5$. The required simulation time was 0.3s. The two flow assumptions did not make any significant difference to any other quantity either, and only the $M = 1$ case was studied further. We show the simulated deposition pattern in figure 5 and simulated toroidal and poloidal profiles in comparison to the measured ones in figures 6 and 7, respectively. The deposition is so localized that 2/3 of the deposited carbon is in fact located toroidally within ± 5 mm from the injection point which is the tile gap in the realistic geometry and only 22% of the injection on the measured area. After achieving the steady state, the injection was turned off and the attached plasma background was applied for another 0.3s to erode the layer, monitoring the evolution of poloidal surface concentration profiles. The erosion is essentially uniform and makes the deposition pattern only narrower without producing the double-maximum structure that is seen in the measured poloidal profiles. However, it is interesting to note that erosion brings the deposit on the measured area down to 9%, which coincides very well with the measured fraction of 10%.

SUMMARY AND DISCUSSION

Surface analysis of two divertor tiles exposed to $^{12}\text{CD}_4$ injection into a detached L-mode plasma is presented. Up to now we have modeled the local carbon transport and deposition with the Onion-Skin Model of DIVIMP and the impurity transport code ERO, reproducing roughly the locally deposited fraction and the toroidal decay of the pattern. The poloidal width of the pattern is significantly underestimated in modelling. The choice of OSM for this work over a fluid model like EDGE2D is a compromise between simplicity and completeness. The highly localized nature of the transport processes relevant for this work suggest that OSM should be at least tested before engaging in much more time-consuming fluid modelling. Clearly we are missing mechanisms contributing to the cross-field transport, e.g. drifts and electric fields were not yet included, but it has been demonstrated that their inclusion into the fluid plasma background model can significantly improve local impurity modelling [10, 11]. Next step of the present modelling will include application of EDGE2D for background plasma generation.

The present experiment features separate phases of hydrocarbon layer deposition and their erosion. The relative intensities of these processes are of great importance for long-term tritium retention. Exact quantification of enhanced re-erosion of deposited layers in tokamaks – in particular divertor plasma conditions – has not yet been done. It is evident from the presented deposition patterns that the interplay of carbon deposition and re-erosion could be quantified in a single experiment in terms of the re-erosion enhancement factor f_{re} . To minimize the uncertainties of such a study, a reliable plasma model is required and plasma the scenario should be maximally compatible to the validity range of the model as well as the requirements of surface analysis.

ACKNOWLEDGEMENTS

This work was supported by EURATOM and carried out within the framework of the European Fusion Development Agreement. The views and opinions expressed herein do not necessarily reflect those of the European Commission. Part of the funding has been obtained from the Academy of Finland. Computing resources have been provided by CSC. CSC is the Finnish IT Centre for Science and is owned by the Ministry of Education.

REFERENCES

- [1]. S. Brezinsek et al., Journal Nuclear Materials **390–391** (2009) 267
- [2]. A. Kirschner, V. Philipps, Journal Winter and U. Kögler, Nuclear Fusion **40** (2000) 989
- [3]. P.C. Stangeby and J.D. Elder, Journal Nuclear Materials **196–198** (1992) 258
- [4]. P.C. Stangeby 2010 These proceedings
- [5]. A. Kreter et al., Journal Nuclear Materials **390–391** (2009) 38
- [6]. P. Wienhold et al., Journal Nuclear Materials **290–293** (2001) 362
- [7]. A. Kirschner et al., Journal Nuclear Materials **328** (2004) 62
- [8]. A. Kirschner et al., Plasma Physics Controlling Fusion **45** (2003) 309
- [9]. M.I. Airila et al., Physics Scripta **T138** (2009) 014021

- [10]. L. Aho-Mantila et al., *Contributors Plasma Physics* **50** (2010) 439
 [11]. L. Aho-Mantila et al., 2010 These proceedings

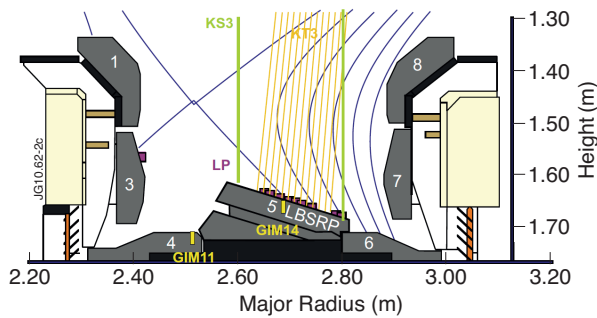


Figure 1: Magnetic configuration and diagnostic coverage in the JET MKII-HD divertor. The outer strike point is positioned on the gas injection location (GIM14) which is embedded in the load-bearing septum replacement tile 5) [1].

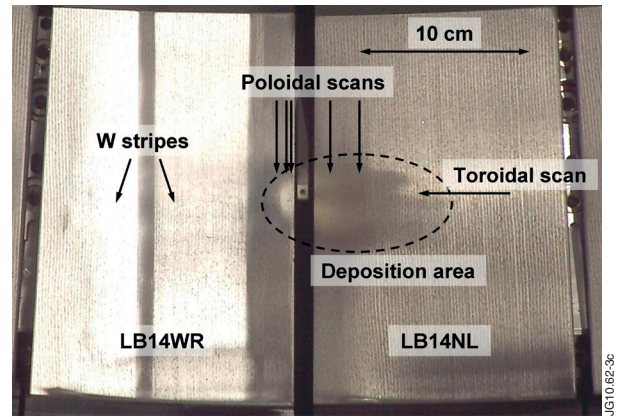


Figure 2: The deposition area extends about 1cm upstream (to left) and 5cm downstream (to right) from the gas injection module. The lines along which poloidal and toroidal profiles were measured are shown by the arrows.

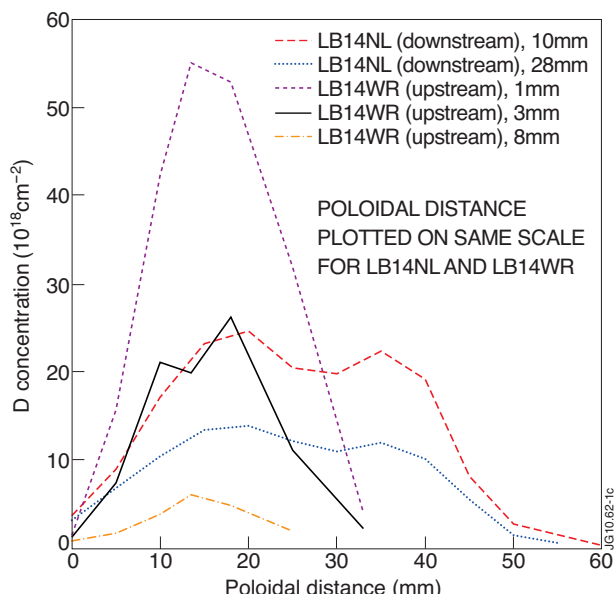


Figure 3: RBS measured surface concentration profiles of deuterium along the lines indicated in figure 2. The double-tail structure visible in figure 2 can be seen as two peaks in the profiles measured from tile LB14NL. The distances given in the legend are measured from the tile edges.

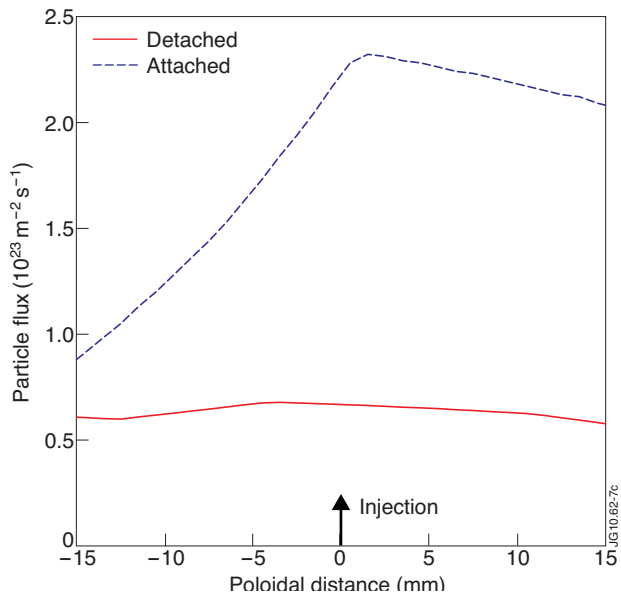


Figure 4: Ion flux to the target from OSM modeled plasma background.

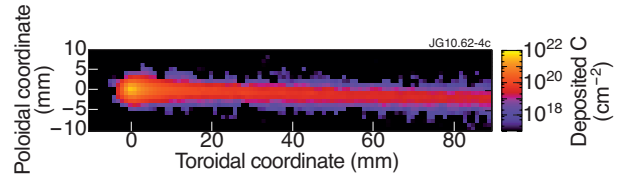


Figure 5: Modeled carbon deposition pattern.

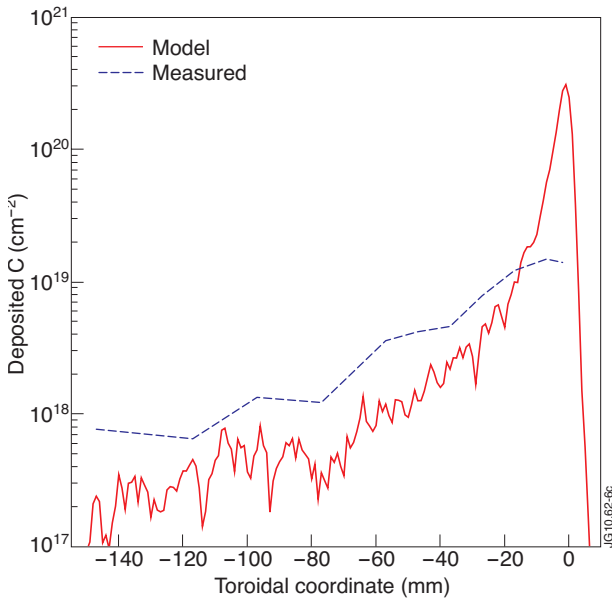


Figure 6: Simulated toroidal carbon surface concentration profile. In comparison to the measurement it is assumed that the D/C ratio in the deposit is 0.4.

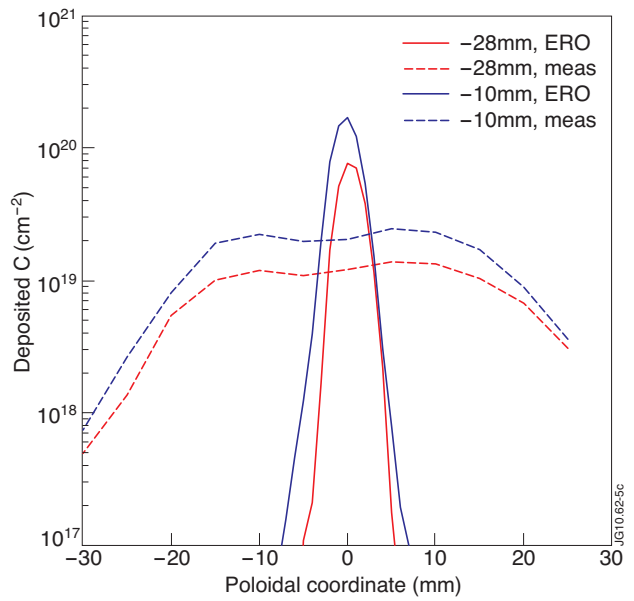


Figure 7: Simulated poloidal carbon surface concentration profile.